Stent and Artery Geometry Determine Intimal Thickening Independent of Arterial Injury

Joseph M. Garasic, MD; Elazer R. Edelman, MD, PhD; James C. Squire, MS; Philip Seifert, MS; Michael S. Williams, BA; Campbell Rogers, MD

Background—Clinical trials show that larger immediate postdeployment stent diameters provide greater ultimate luminal size, whereas animal data show that arterial injury and stent design determine late neointimal thickening. At deployment, a stent stretches a vessel, imposing a cross-sectional polygonal luminal shape that depends on the stent design, with each strut serving as a vertex. We asked whether this design-dependent postdeployment luminal geometry affects late neointimal thickening independently of the extent of strut-induced injury.

Methods and Results—Stainless steel stents of 3 different configurations were implanted in rabbit iliac arteries for 3 or 28 days. Stents designed with 12 struts per cross section had 50% to 60% less mural thrombus and 2-fold less neointimal area than identical stents with only 8 struts per cross section. Sequential histological sectioning of individual stents showed that immediate postdeployment luminal geometry and subsequent neointimal area varied along the course of each stent subunit. Mathematical modeling of the shape imposed by the stent on the artery predicted late neointimal area, based on the re-creation of a circular vessel lumen within the confines of the initial stent-imposed polygonal luminal shape.

Conclusions—Immediate postdeployment luminal geometry, dictated by stent design, determines neointimal thickness independently of arterial injury and may be useful for predicting patterns of intimal growth for novel stent designs. **(*Circulation*. 2000;101:812-818.)**

Key Words: stents ■ restenosis ■ angioplasty ■ pathology

The advantages of stents over angioplasty include larger acute gains in luminal diameter and better long-term patency and clinical outcomes.[1,2] Nevertheless, stents provoke greater absolute late luminal loss than angioplasty[1,3–5] and carry the additional risk of thrombosis.[6] Better understanding of mechanical and biological contributors to thrombosis has prompted changes in clinical practice.[7] In contrast, no strategy has been proved clinically effective at reducing the neointimal hyperplasia of in-stent restenosis.[8] A central element in understanding in-stent restenosis is how stent design may affect neointimal growth. One aspect of stent-induced damage is strut-imposed vascular injury, which dictates the extent of intimal thickening in experimental animals.[9,10] Design alterations that limit injury modulate neointimal hyperplasia.[11,12] Meanwhile, clinical evidence suggests that larger immediate postdeployment dimension is the primary predictor of late luminal area, independent of stent design.[3–5]

At deployment, stent struts provide a frame over which the lumen is stretched, assuming a polygonal shape, with each strut marking a vertex. The geometry depends on stent design and varies along the length of a single stent. To test the hypothesis that acute stent-imposed luminal geometry affects vascular repair, stents were constructed to alter luminal geometry with minimal effect on deep injury. Using sequential histological sectioning, we examined whether initial stent-imposed lumen shape affects regional neointimal thickening. A mathematical model was constructed to examine whether these effects occurred in a predictable fashion. Elucidating effects of stent design on initial stent-imposed luminal geometry and biological sequelae may allow novel strategies for device design and use. Furthermore, the plethora of stent designs now available makes understanding and modeling of precise interactions between stent and artery essential.

Methods

Surgical Procedure

New Zealand White rabbits (Covance Products, Denver, Pa), 3.5 to 4 kg, were fed rabbit chow and water. Aspirin (0.07 mg/mL, Sigma Chemical Co) was added to the drinking water 1 day before surgery for a dosage of $\approx 5\ mg \cdot kg^{-1} \cdot d^{-1}$ and was maintained throughout the

Received June 1, 1999; revision received August 6, 1999; accepted August 26, 1999.

From the Department of Medicine (Cardiac Catheterization Laboratory and Coronary Care Unit, Brigham and Women's Hospital), Harvard Medical School, Boston, Mass (J.M.G., E.R.E., C.R.); the Harvard-MIT Division of Health Sciences and Technology, Massachusetts Institute of Technology, Cambridge, Mass (E.R.E., J.C.S., P.S., C.R.); and Medtronic/Arterial Vascular Engineering, Santa Rosa, Calif (M.S.W.).

M.S. Williams is an employee of Medtronic/Arterial Vascular Engineering, whose stents are the subject of this study.

Correspondence to Joseph Garasic, MD, Brigham and Women's Hospital, 75 Francis St, Boston, MA 02115. E-mail jmgarasic@bics.bwh.harvard.edu

Circulation **is available at http://www.circulationaha.org**

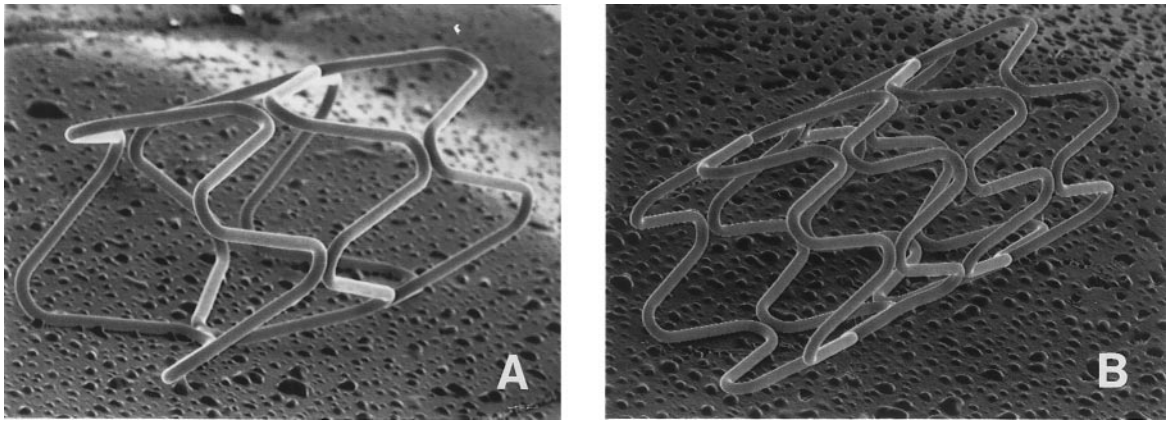

Figure 1. Scanning electron micrographs (magnification ×18) show stents of 8-strut (A) and 12-strut (B) designs after balloon expansion.

postoperative period. Animals were anesthetized with ketamine (35 mg/kg IM, Fort Dodge Laboratories) and xylazine (5 mg/kg IM, Miles Inc). As previously described,[12,13] we performed bilateral iliac artery denudation using a 3F embolectomy catheter (Baxter Health-Care Corp). A stent mounted on a 3-mm angioplasty balloon (Arterial Vascular Engineering) was passed retrogradely into each iliac artery and expanded (15 seconds, 8 atm). Iliac arteries of rabbits in this weight range are 2.5 to 2.75 mm in diameter, yielding balloon:artery ratios of 1.1 to 1.2:1.[12–14] At the time of stent deployment, rabbits received a single bolus of heparin (100 U/kg, Elkin-Sinn Inc). All animal care was in accordance with institutional guidelines.

Steel stents of 3 designs were used. Stents were of a simple multicrowned configuration with either 8 (Figure 1A) or 12 (Figure 1B) struts per cross section. Stents of the 12-strut design were 8 mm long (four 2-mm segments), and stents of the 8-strut design were 9 mm long (three 3-mm segments). Variations in strut thickness were tested as well, with stent struts of the 12-strut design being either 125 or 200 μm thick. Struts of the 8-strut design were 200 μm thick. In vitro expansion of all 3 stent designs showed an outer dimension of 3.4 mm for 200-μm-thick stents of either design and 3.3 mm for 125-μm-thick 12-strut stents.

Tissue Processing

Four stents of each design were implanted for 3 days, and 4 each for 28 days. To label proliferating cells, all animals received bromodeoxyuridine (BrdU) (50 mg/kg IV, Sigma) 1 hour before they were euthanized. Under anesthesia with pentobarbital sodium, inferior vena caval exsanguination was followed by perfusion with Ringer's lactate solution via left ventricular puncture. Both iliac arteries were excised and fixed by immersion in Carnoy's solution (60% methanol, 30% chloroform, and 10% glacial acetic acid). Intact stented arterial segments were embedded in a modified methacrylate resin formulation (Sigma Chemical Co) polymerized at −20°C. Before sectioning, high-resolution radiographs of embedded stented arteries were taken in 2 orthogonal views with a mammography unit, and the external stent diameter was measured at the proximal end, the middle, and the distal end with digital calipers. Cross-sectional planes were then sawed out and sectioned at 5-μm thickness with a tungsten carbide knife as previously described.[15,16] Cross sections were taken from each end and the middle of each stented artery.

To study neointimal hyperplasia along the length of a single stent subunit, sequential 5-μm sections from the middle of two 8-strut stents were taken at 100-μm intervals. This allowed study of neointimal responses along one half of 3-mm segments, with the subsequent half (1.5 mm) being a mirror image of the studied segment.

Histological Analysis

Histological sections were stained with Verhoeff's tissue elastin stain or hematoxylin and eosin. Areas of neointima, adherent mural thrombus, lumen, internal elastic lamina (IEL), and external elastic lamina were measured by computer-assisted digital planimetry as previously described.[12] Stent-induced injury score was graded for each cross section.[9,10]

Cellular responses 3 and 28 days after stent implantation were also studied. In proximal, middle, and distal sections of each stented artery, mononuclear inflammatory cells adherent to the lumen were counted.[12,15,16] Macrophages were identified immunohistochemically with a species-specific antibody (RAM-11, Dako Co).[15,16] Proliferating neointimal cells were quantified by BrdU incorporation (anti-BrdU, Dako Co). Sections were incubated with primary antibody and then biotinylated species-specific secondary antibody (Vector Laboratories Inc). Positive cells were detected by avidin-biotin-peroxidase or –alkaline phosphatase kits (Vector Laboratories Inc). Immunohistochemically identified monocytes/macrophages or proliferating cells were counted and their densities calculated.

Mathematical Modeling

When a stent is initially deployed, its struts provide a scaffold over which the intima is tightly stretched. The lumen therefore initially assumes the geometric shape of a polygon, with the struts marking each vertex. We sought to determine whether eventual lumen shape and the area of neointimal growth late after stent implantation is a function of the shape of this polygon and the largest circular lumen that can be inscribed within it.

The stents we considered can be closely modeled in a straight vessel as a series of linked diamonds as shown in Figure 2. The strut locations for this design at any given cross section are uniquely determined by 3 variables: the number of diamonds, N, needed to traverse the lumen circumference (N=4 in Figure 2 and in the 8-strut stents used in this study, N=6 in the 12-strut stents used in this study); the balloon radius, R_b; and the longitudinal position α of the cross section. The strut configuration in Figure 2 across section A stretches the lumen into the shape of a square; across section C into an octagon; and between these regions, at section B, into an 8-sided shape consisting of 4 grouped pairs of vertices. The distance from A to C is measured with the normalized variable α, which is given the value 0 at cross section A and 1 at cross section C. Because the paired strut groupings between A and C are the same as between C and the following A with a 90° rotation, analysis was completed only on the region from A to C.

One can derive the equations governing predicted neointimal area for any N, R_b, and α from examination of Figure 2. A stent whose circumference is spanned by N circumferential diamond-shaped elements will have 2N struts showing at each cross section, (with an exception at $\alpha=0$, where strut pairs join). These 2N struts are separated by 2 angles, the larger θ_1 and the smaller θ_2 (Figure 2). At $\alpha=0$, $\theta_1=2\pi/N$ and $\theta_2=0$. At $\alpha=1$, $\theta_1=\theta_2=\pi/N$. The area of the

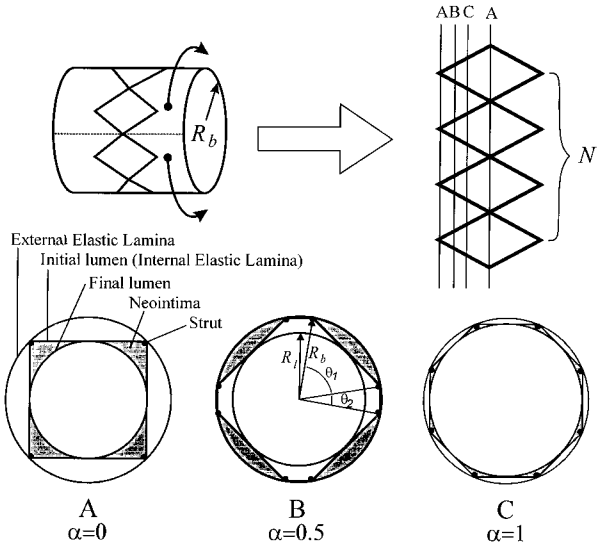

Figure 2. Schematic of stent strut geometry as a series of linked diamonds. N indicates number of diamonds encircling circumference of stent; R_b, postdeployment radius; and R_i, radius of best-fit circle inscribed in stent-imposed geometry. Strut configuration at different points along same stent imposes on arterial lumen square (section A), octagonal (section C), or 8-sided polygon (section B) shapes. Strut distribution varies in a continuous fashion along a single stent subunit (A through C) as reflected by continuous variable α (range: $\alpha=0$ to 1). θ_1 and θ_2 are angles between adjacent struts.

polygon inscribed by the stent struts (A_p) can then be calculated as follows:

$$(1) \qquad A_p=\frac{R_b^2 N}{2}[\sin\theta_1(\alpha)+\sin\theta_2(\alpha)].$$

The radius (R_i) of the largest circle that can be inscribed within this polygon can be calculated as

$$(2) \qquad R_i=R_b\cos[\theta_1(\alpha)/2],$$

and the predicted area of neointimal hyperplasia (NIH) as a function of R_b, N, and α can be calculated as acute lumen area (Equation 1) minus eventual luminal area (πR_i^2):

$$(3) \qquad \mathrm{NIH}(R_b,N,\alpha)$$
$$=\frac{R_b^2}{2}\{N[\sin\theta_2(\alpha)+\sin\theta_1(\alpha)]-\pi[1+\cos\theta_1(\alpha)]\}.$$

This equation predicts that neointimal growth will vary in a cyclic manner along the length of the stent, allowing comparison with histological data from sequential sections taken from N=4 (8-strut) stents. To determine the mean neointimal area, independent of α, within a stent for any N and R_b, Equation 3 can be integrated over all values of α, yielding

TABLE 2. Histomorphometric Analysis 28 Days After Stent Implantation

	8 Strut 200 μm	12 Strut 200 μm	12 Strut 125 μm
Intima, mm²	1.54±0.13*	0.80±0.08	0.87±0.15
Lumen, mm²	2.66±0.17†	3.73±0.18	3.63±0.12
IEL, mm²	4.20±0.14	4.53±0.12	4.50±0.14
EEL, mm²	4.67±0.12	4.68±0.10	4.62±0.15
Injury score	0.34±0.03‡	0.26±0.08	0.25±0.02

EEL indicates external elastic lamina.
*$P<0.002$ vs 12-strut 200-μm stent, $P<0.005$ vs 12-strut 125-μm stent.
†$P<0.001$ vs 12-strut 200-μm stent, $P<0.004$ vs 12-strut 125-μm stent.
‡$P=0.30$ vs 12-strut 200-μm stent, $P=0.27$ vs 12-strut 125-μm stent.

$$(4) \qquad \mathrm{NIH}_{\mathrm{mean}}(R_b,N)$$
$$=\frac{R_b^2}{2\pi}\left[N\pi\left(\sin\frac{\pi}{N}-\sin\frac{2\pi}{N}\right)+N^2\left(1-\cos\frac{2\pi}{N}\right)-\pi^2\right].$$

We hypothesized that stent-induced neointimal formation reflects geometric issues analyzed in this article as well as nongeometric issues, such as underlying vessel composition, stent material, and the extent of deep injury. These nongeometric issues do not change in a regular graded fashion along the length of a single stent and thus contribute a constant baseline term to the equation of predicted neointimal area on which geometrically determined fluctuations are imposed. We therefore offset the predicted neointimal areas obtained from Equation 3 when plotting the resultant modeled data against our experimentally obtained sequential-section data.

Statistics

All data are presented as mean±SEM. Comparisons between treatment groups used ANOVA with Bonferroni-Dunn correction for multiple comparisons.

Results

Stent Dimensions

Measurement of external stent diameter for all specimens before sectioning showed full expansion at proximal, middle, and distal segments for all 3 stent designs and no differential recoil or end-tapering in any design over time (Table 1).

Vascular Injury

Deep injury to the arterial wall at the time of stent deployment is known to correlate closely with late neointimal thickening in experimental models.[9,10,12] Our experiments were designed to minimize differences in stent-imposed arterial injury, allowing isolated study of luminal shape as a factor in repair. Measured injury scores were low and did not differ significantly between stent designs (Table 2).

TABLE 1. Outer Diameter of Stents 3 or 28 Days After Implantation

	3 Days			28 Days		
	8 Strut 200 μm	12 Strut 200 μm	12 Strut 125 μm	8 Strut 200 μm	12 Strut 200 μm	12 Strut 125 μm
Proximal	2.69±0.07	2.75±0.11	2.73±0.03	2.72±0.05	2.67±0.05	2.57±0.07
Middle	2.64±0.04	2.76±0.12	2.67±0.04	2.57±0.02	2.67±0.02	2.62±0.08
Distal	2.62±0.05	2.69±0.07	2.65±0.05	2.64±0.03	2.55±0.02	2.58±0.06

Values are in millimeters.
P=NS for all comparisons.

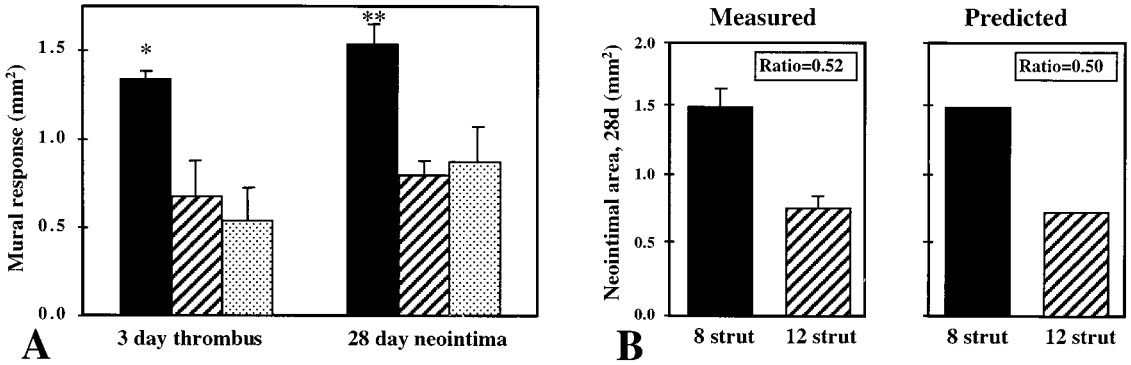

Figure 3. A, Area of mural thrombus 3 days and neointimal area 28 days after balloon injury and stent deployment. Solid bars indicate 8-strut 200-μm stents; hatched bars, 12-strut 200-μm stents; and stippled bars, 12-strut 125-μm stents. *$P<0.004$ vs 12-strut 125-μm and $P<0.01$ vs 12-strut 200-μm design; **$P<0.005$ vs 12-strut 125-μm design and $P<0.002$ vs 12-strut 200-μm design. Altered strut thickness did not significantly affect thrombus or neointimal area (P=NS for 12-strut 125-μm vs 12-strut 200-μm design at 3 or 28 days). B, A 0.52 ratio of measured neointimal area after 28 days in 12-strut 200-μm stents (hatched bar) vs 8-strut 200-μm stents (solid bar). Ratio of predicted neointimal areas between these same stent designs derived from Equation 4 is 0.50.

Thrombosis and Mural Thrombus Burden

No stents were found to be completely thrombosed at harvest. Variable amounts of adherent mural thrombus were present after 3 days, localized around stent struts. Despite similar degrees of vascular injury, 3-day mural thrombus burden (Figure 3A) was reduced 50% to 60% by increasing strut number from 8 to 12 (mural thrombus area: 1.34 ± 0.04 mm^2 for 8-strut stent; 0.54 ± 0.19 mm^2 for 12-strut 125-μm stent, $P<0.004$ compared with 8-strut; 0.67 ± 0.19 mm^2 for 12-strut 200-μm stent, $P<0.001$ compared with 8-strut, P=NS compared with 12-strut 125-μm).

Neointimal Hyperplasia

Neointimal hyperplasia was examined for stents of different strut number and thickness but similar arterial injury scores. Twelve-strut stents displayed 2-fold less neointima (Table 2, Figures 3A and 4) than 8-strut stents (intimal area: 1.54 ± 0.13 mm^2 for 8-strut stents; 0.87 ± 0.15 mm^2 for 12-strut 125-μm stents, $P<0.005$ compared with 8-strut; 0.80 ± 0.08 mm^2 for 12-strut 200-μm stents, $P<0.002$ compared with 8-strut, P=NS compared with 12-strut 125-μm; Table 2, Figures 3A and 4). Lumen areas followed a pattern inverse to neointimal areas (Table 2). Furthermore, there was a trend toward greater IEL areas in 12-strut stents, reflecting the greater circumference inscribed by a 12-strut stent than an 8-strut stent for any fixed stent diameter (Table 2). From Equation 4, the predicted ratio for neointimal hyperplasia between 8-strut and 12-strut stents was 0.50. The same ratio calculated with measured values of neointimal area was 0.52 (Figure 3B).

Inflammatory and Proliferative Indices

The presence of luminally adherent monocytes correlates with neointimal thickening in this model of stent-induced injury.[12,15–17] At 28 days, few luminal monocytes were present: 19 ± 4 monocytes per section in 8-strut stents, 11 ± 9 in 12-strut 200-μm stents, and 12 ± 4 in 12-strut 125-μm stents (P=NS for all comparisons). More RAM-11–positive macrophages were identified among stents of the 12-strut design: $0.47\pm0.17\%$ in 8-strut stents; $1.07\pm0.44\%$ in 12-strut 200-μm stents ($P<0.04$ compared with 8-strut); and $1.07\pm0.15\%$ in 12-strut 125-μm stents ($P<0.04$ compared with 8-strut). Increasing strut number from 8 to 12 was also associated with more proliferating cells: BrdU positivity was $0.04\pm0.01\%$ in the 8-strut group, $0.15\pm0.07\%$ in the 12-strut 200-μm group ($P<0.02$ compared with 8-strut), and $0.15\pm0.02\%$ in the 12-strut 125-μm group ($P<0.02$ compared with 8-strut 200-μm). Most BrdU-positive cells were of monocyte-macrophage lineage in the peristrut regions, explaining the slightly higher numbers of these cells in 12-strut stents.

Sequential Sectioning and Mathematical Modeling

To examine a potential mechanism whereby strut-vessel geometric interactions may modulate neointimal thickening, sequential sections were taken at 100-μm intervals along two 8-strut stents harvested after 28 days. This allowed examination of neointimal thickening as strut configuration varied. Within any stented segment, radial strut distribution varied depending on the point at which the sections were taken. In sections taken near the beginning of the stent segment, the IEL was stretched between the 4 cusps in a square design, and

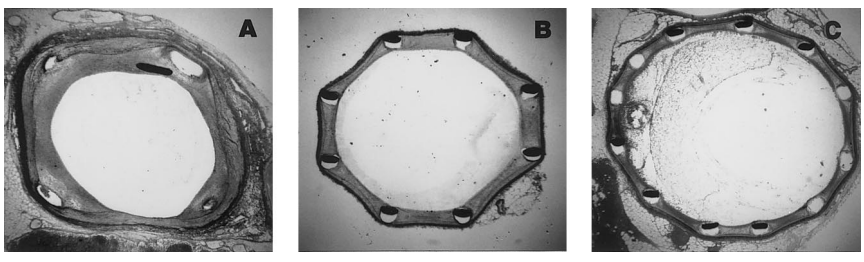

Figure 4. Photomicrographs show rabbit iliac artery cross sections (magnification $\times4$) 28 days after balloon injury and stent deployment. A, An 8-strut stent at confluence of struts, where 4 struts impose a square form on IEL; B, 8-strut stent at point at which struts are evenly spaced imposes an octagonal shape on IEL; and C, 12-strut stent in which struts are evenly spaced.

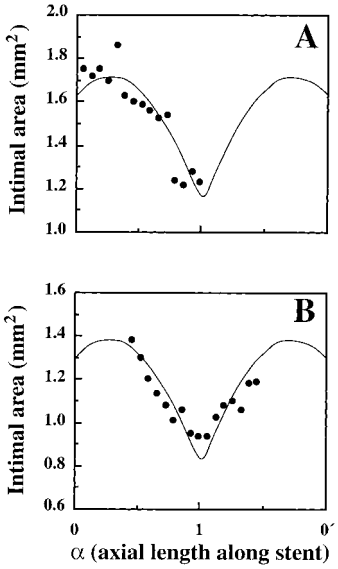

Figure 5. Measured intimal area (●) in serial histological sections taken at different points (α) along two 8-strut 200-μm stent segments (A and B). Measured values correspond closely to predicted neointimal areas derived from Equation 3 (solid lines). A, With increasing regularity of strut distribution (α from 0 to 1), neointimal area falls to a nadir. B, As struts again become unevenly spaced (α from 1 to 0′), neointimal area rises.

these sections showed a large amount of neointimal hyperplasia (Figure 4A). Sections taken at the other end of the segment near 8 equidistant, radially distributed struts showed an octagonal IEL and markedly less neointima (Figure 4B). These values and all in between were measured and plotted as a function of distance along the stent segment (Figure 5). Using Equation 3 above, we calculated predicted neointimal area for N=4 (Figure 5). These derived and measured values showed that neointimal area fell and lumen size rose as struts became more numerous and more evenly distributed. As the cycle then repeated and struts again became less evenly spaced, neointimal area rapidly began to rise again. In both sequentially sectioned stents, the predicted neointimal area, derived by use of a geometric model to inscribe a largest, best-fit circular lumen within stent-imposed initial lumen geometry, closely approximated histologically measured values (Figure 5).

Discussion

Studies of neointimal thickening after vascular stenting have identified deep vessel laceration in animals[9–12] and early gains in luminal dimension in humans[3–5] as determinants of late luminal size. There has been debate as to whether these 2 paradigms are reconcilable. At deployment, a stent imposes on the lumen a polygonal shape that depends on stent design, with each strut at a vertex. We asked whether this design-dependent postdeployment luminal geometry affects late neointimal thickening independent of strut-induced injury. We present a new model of experimentally induced intimal thickening whereby immediate postdeployment 3D luminal geometry determines eventual lumen size. These data demonstrate how, even in the absence of deep arterial injury, stent design can markedly affect lumen shape and produce distinctly different degrees and patterns of intimal thickening.

With stents differing in strut number but imposing similar injury scores, isolated investigation of the effects of altering initial lumen shape was possible. Altering lumen shape by increasing the number of struts per cross section from 8 to 12 was associated with a 50% to 60% drop in mural thrombus burden after 3 days and a 2-fold reduction in neointimal thickening after 28 days. In contrast, changing only strut thickness from 125 to 200 μm had no significant impact on early luminal thrombus or late intimal thickening. There was no evidence of differential stent expansion or tapering. Computer-aided mathematical modeling used to inscribe a largest, best-fit circular lumen within the confines of different stent-imposed acute luminal configurations accurately predicted different degrees of neointimal thickening. Detailed sequential sectioning of 8-strut stent segments showed that as struts became more numerous and evenly distributed, neointimal area fell and lumen size rose in a completely predictable manner.

These findings may elucidate biological mechanisms of neointimal hyperplasia after vascular stenting. Restoration of luminal circularity may be driven by elements of arterial strain or flow characteristics. Stent-imposed strain for a vessel of any given size will increase as a function of increasing stent diameter. At the same diameter, stents with greater strut number will produce larger lumen circumferences and therefore increase chronic stent-imposed strain. This is suggested by data from our experiments, which show a trend toward greater IEL areas in 12-strut stents. Increasing vascular strain may affect cellular orientation and enhance cell proliferation.[18–20] Thus, there was no reduction in chronic vascular strain with increasing strut number that would explain the reduction in neointimal thickening seen in the 12-strut stents. Conversely, for a vessel of fixed size, greater interstrut distances are associated with greater acute strain imposed on the vessel wall by the balloon during stent expansion.[21]

In contrast, altered stent-imposed fluid dynamics may well explain our findings. Several groups have examined the fluid dynamics governing blood flow through stented arteries.[22–24] Their discoveries of regions of turbulence and/or stagnation in the immediate vicinity of stent struts provide a basis for the observation that restoring the lumen to a circular shape will optimize fluid flow characteristics at the blood/tissue interface. Platelet and inflammatory cell adhesion and activation may be less in settings of more laminar flow within the lumen of more circular stented vessels.

Our data show that less thrombus is present in stents of the 12-strut design than the 8-strut design and there is an accompanying decrement in neointimal thickening at 28 days. Several investigators have suggested that early thrombus deposition and late intimal thickening may be linked in experimental models.[9,10,25] Alternatively, a common mechanism, most likely flow-mediated, may underlie both processes, driving thrombus deposition as well as intimal thickening at different phases of repair.

The trend toward fewer luminal monocytes among 12-strut stents versus 8-strut stents at 28 days correlates with the

accompanying difference in neointimal thickening, as reported previously.[12,13,15,16] In the present study, however, tissue macrophage numbers and proliferative indices were increased among stents of the 12-strut design. This apparent paradox may be explained by the observation that macrophages, monocytes, and giant cells cluster around stent struts. As strut number increases from 8 to 12, the proportion of neointima rich in tissue inflammatory cells increases. In contrast to luminally adherent cells, tissue cells reflect earlier recruitment and may not presage delayed neointimal thickening. Nevertheless, greater late neointimal growth, after 28 days, in the 12-strut stents cannot be ruled out from our experiments.

Altering stent strut configuration and number has practical effects on the clinical use of vascular stents. Increasing strut number and regularity of strut distribution provides a more circular vascular lumen and is associated with a smoother, more homogeneous arteriographic contour. Although our data suggest that variation in strut thickness within the range studied had no significant impact on the biological end points we investigated, in clinical use, thicker struts enhance radiopacity and radial strength, 2 favorable stent characteristics. It is possible that the beneficial effects of increased strut number and near-circular postdeployment lumen shape outweigh any detrimental effects of increased stent mass. There may be a limit, however, to the benefits of this biological effect, and the detrimental effects of increasing strut number or thickness may eventually overcome the beneficial effect of a circular postdeployment lumen shape.

Study Limitations

The stents studied differed in length by 1 mm (8 versus 9 mm) out of the necessity to achieve comparable hoop strength. This difference is unlikely to have a significant biological consequence, because these short stents were deployed in long, nontapering vessels. Furthermore, we documented stent-vessel interactions at various points along each stent, which would be unaffected by minor differences in stent length. In mathematical modeling, we made a simplifying assumption in the geometric derivations for intimal area concerning the behavior of the arterial wall. Because the arterial wall has some thickness, it may not stretch into straight-line segments joining the strut vertices, as we assumed. Instead, the media will resist compression by forcing the interstrut luminal region to bow slightly inward. This effect contributes negligible error when the thin-walled iliac vessels of the rabbit model are used but may be more consequential in thicker muscular coronary arteries or abnormal atherosclerotic vessels. Finally, in vivo imaging of stent sizes was not obtained, although ex vivo test expansions and postmortem measurement of explanted stents showed no differences in diameters between designs.

Conclusions

Clinical trials support the paradigm that a larger postdeployment stent diameter provides greater ultimate luminal size, although an effect of stent design on clinical restenosis has not been proved. Animal data, conversely, show that arterial injury as dictated by stent design affects late neointimal thickening. We describe a new model of intimal thickening dependent only on lumen size and shape as determined by stent design. Immediate postdeployment 3D luminal geometry and recreation of a circular vessel lumen within the confines of this initial stent-vessel shape determine eventual lumen size. These data attest to the importance of stent design as a predictor of biological outcomes and may serve to guide future stent design and the choice between stents of differing designs within the clinical arena.

Acknowledgments

This work was supported in part by grants from the NIH (GM/HL-49039 and HL-60407 to Dr Edelman and HL-03104 to Dr Rogers). Dr Edelman is an Established Investigator of the American Heart Association. We are grateful to Cindy Richmond for expert technical assistance and to Dr Jeffrey J. Popma for critical review of the manuscript.

References

1. Serruys PW, de Jaegere P, Kiemeneij F, Macaya C, Rutsch W, Heyndrickx G, Emanuelsson H, Marco J, Legrand V, Materne P, Belardi J, Sijwart U, Colombo A, Goy J, van den Heuvel P, Delcan J, Morel M. A comparison of balloon-expandable-stent implantation with balloon angioplasty in patients with coronary artery disease. *N Engl J Med*. 1994; 331:489–495.
2. Fischman DL, Leon MB, Baim DS, Schatz RA, Savage MP, Penn IM, Detre K, Veltri L, Ricci DR, Nobuyoshi M, Cleman MW, Heuser RR, Almond D, Teirstein PS, Fish RD, Colombo A, Brinker J, Moses J, Shaknovich A, Hirshfeld J, Bailey S, Ellis S, Rake R, Goldberg S. A randomized comparison of coronary artery-stent placement and balloon angioplasty in the treatment of coronary artery disease. *N Engl J Med*. 1994;331:496–501.
3. Kuntz RE, Safian RD, Levine MJ, Reis GJ, Diver DJ, Baim DS. Novel approach to the analysis of restenosis after the use of three new coronary devices. *J Am Coll Cardiol*. 1992;19:1493–1499.
4. Kuntz RE, Safian RD, Carrozza JP, Fishman RF, Mansour M, Baim DS. The importance of acute luminal diameter in determining restenosis after coronary atherectomy or stenting. *Circulation*. 1992;86: 1827–1835.
5. Kuntz RE, Gibson CM, Nobuyoshi M, Baim DS. Generalized model of restenosis after conventional balloon angioplasty, stenting, and directional atherectomy. *J Am Coll Cardiol*. 1993;21:15–25.
6. Hasdai D, Garratt KN, Holmes DR, Berger PB, Schwartz RS, Bell MR. Coronary angioplasty and intracoronary thrombolysis are of limited efficacy in resolving early intracoronary stent thrombosis. *J Am Coll Cardiol*. 1996;28:361–367.
7. Schömig A, Neumann F-J, Kastrati A, Schühlen H, Blasini R, Hadamitzky M, Walter H, Zitzmann-Roth E-M, Richart G, Alt E, Schmitt C, Ulm K. A randomized comparison of antiplatelet and anticoagulant therapy after the placement of coronary-artery stents. *N Engl J Med*. 1996;334:1084–1089.
8. Hoffmann R, Mintz GS, Dussaillant GR, Popma JJ, Pichard AD, Satler LF, Kent KM, Griffin J, Leon MB. Patterns and mechanisms of instent restenosis: a serial intravascular ultrasound study. *Circulation*. 1996;94:1247–1254.
9. Schwartz RS, Holmes DH, Topol EJ. The restenosis paradigm revisited. *J Am Coll Cardiol*. 1992;20:1284–1293.
10. Schwartz RS, Huber KC, Murphy JG, Edwards WD, Camrud AR, Vlietstra RE, Holmes DR. Restenosis and proportional neointimal response to coronary artery injury. *J Am Coll Cardiol*. 1992;19: 267–274.
11. Barth KH, Virmani R, Froelich J, Takeda T, Lossef SV, Newsome J, Jones R, Lindisch D. Paired comparison of vascular wall reactions to Palmaz stents, Strecker tantalum stents, and Wallstents in canine iliac and femoral arteries. *Circulation*. 1996;93:2161–2169.
12. Rogers C, Edelman ER. Endovascular stent design dictates experimental restenosis and thrombosis. *Circulation*. 1995;91:2995–3001.
13. Rogers C, Karnovsky MJ, Edelman ER. Inhibition of experimental neointimal hyperplasia and thrombosis depends on the type of vascular injury and the site of drug administration. *Circulation*. 1993; 88:1215–1221.

14. Van Belle E, Tio FO, Couffinhal T, Maillard L, Passeri J, Isner JM. Stent endothelialization. *Circulation*. 1997;95:438–448.
15. Rogers C, Parikh S, Seifert P, Edelman ER. Endogenous cell seeding. *Circulation*. 1996;94:2909–2914.
16. Rogers C, Welt FGP, Karnovsky MJ, Edelman ER. Monocyte recruitment and neointimal hyperplasia in rabbits. *Arterioscler Thromb Vasc Biol*. 1996;16:1312–1318.
17. Rogers C, Edelman DI, Simon DI. A mAb to the B2-leukocyte integrin Mac-1 (CD11b/CD18) reduces intimal thickening after angioplasty or stent implantation in rabbits. *Proc Natl Acad Sci U S A*. 1998;95:10134–10139.
18. Cheng GC, Briggs WH, Gerson DS, Libby P, Grodzinsky AJ, Gray ML, Lee RT. Mechanical strain tightly controls fibroblast growth factor-2 release from cultured human vascular smooth muscle cells. *Circ Res*. 1997;80:28–36.
19. Buck RC. Behavior of vascular smooth muscle cells during repeated stretching of the substratum in-vitro. *Atherosclerosis*. 1983;46:217–223.
20. Cheng GC, Libby P, Grodzinsky AJ, Lee RT. Induction of DNA synthesis by a single transient mechanical stimulus of human vascular smooth muscle cells. *Circulation*. 1996;93:99–105.
21. Rogers C, Tseng DY, Squire JC, Edelman ER. Balloon-artery interactions during stent placement. *Circ Res*. 1999;84:378–383.
22. Aenis M, Stancampio AP, Wakhloo AK, Lieber BB. Modeling of flow in a straight stented and nonstented side wall aneurysm model. *J Biomech Eng*. 1997;119:206–212.
23. Lieber BB, Stancampio AP, Wakhloo AK. Alteration of hemodynamics in aneurysm models by stenting. *Ann Biomed Eng*. 1997;25:460–469.
24. Peacock J, Hankins S, Jones T, Lutz R. Flow instabilities induced by coronary artery stents. *J Biomech*. 1995;28:17–26.
25. Ip JH, Fuster V, Badimon L, Badimon J, Taubman MB, Chesebro JH. Syndromes of accelerated atherosclerosis. *J Am Coll Cardiol*. 1990;15:1667–1687.